ON THE CAPACITY OF OFDM-BASED MULTI-ANTENNA SYSTEMS

Helmut Bölcskei, David Gesbert, and Arogyaswami J. Paulraj

Information Systems Laboratory, Stanford University
Packard 223, 350 Serra Mall, Stanford, CA 94305-9510
Phone: (650)-724-3640, Fax: (650)-723-8473, email: bolcskei@rascals.stanford.edu

Abstract—We compute the capacity of wireless Orthogonal Frequency Division Multiplexing (OFDM)-based spatial multiplexing systems in delay spread environments. Introducing an abstract model to characterize the statistical properties of the space-time channel, we provide a Monte-Carlo method for estimating the capacity cumulative distribution function, expected capacity, and outage capacity for the case where the channel is unknown at the transmitter and perfectly known at the receiver. We study the influence of the propagation environment and system parameters on capacity, and we apply our method to spatial versions of standard channels taken from the GSM recommendations. This allows us to make statements about achievable data rates of OFDM-based spatial multiplexing systems operating in practical broadband propagation environments.

1. INTRODUCTION AND OUTLINE

The use of multiple antennas at both the base transceiver station (BTS) and the subscriber unit (SU) in a wireless system has recently been shown to have the potential of achieving extraordinary bit rates [1]-[4]. So far, most of the investigations on the capacity of such multi-antenna systems have been confined to narrowband flat-fading channels [2, 3, 5, 6, 7].

In this paper, we compute the capacity of Orthogonal Frequency Division Multiplexing (OFDM)-based spatial multiplexing systems [1, 4, 8] employing blind transmission (i.e. the channel is unknown at the transmitter and known at the receiver) in realistic broadband propagation environments. Based on work reported in [9, 10], we first introduce a new space-time channel model appropriate for multiple transmit and multiple receive antennas. Using this model, we then devise a Monte-Carlo method for estimating the capacity cumulative distribution function (cdf), expected capacity, and outage capacity of the spatial multiplexing system, and we provide bounds on capacity. Our channel model reveals the influence of propagation environment parameters such as the amount of delay spread, angles of arrival, scattering radius, and path attenuations as well as system parameters such as the number of antennas and antenna spacing on capacity. Using a parametric channel model, capacity expressions for the delay spread case have been derived previously in [4, 8]. However, our channel model captures the effects of spatial fading correlation, diffuse scattering, and scattering radius on capacity, and is therefore fundamentally different from the one proposed in [4, 8]. Furthermore, in the channel model used in [4, 8] each path can only be a rank 1 contributor to capacity[1], whereas in our model this rank depends on the propagation environment and system parameters.

The rest of this paper is organized as follows. In Section 2, we introduce the new space-time channel model. In Section 3, OFDM-based spatial multiplexing is briefly described. In Section 4, we derive an expression for the capacity distribution of OFDM-based spatial multiplexing systems, and we provide bounds on capacity. In Section 5, we describe a Monte-Carlo based method for estimating the expected capacity, outage capacity, and the capacity cdf and we provide simulation results.

2. SPACE-TIME CHANNEL MODEL

In this section, we shall introduce a new model for stochastic space-time delay spread channels based on a physical description of the propagation environment.

Propagation Scenario. We assume that the SU is surrounded by local scatterers so that fading at the SU-antennas is spatially uncorrelated. The BTS, however, is unobstructed and no local scattering occurs. Therefore, spatial fading at the BTS will be correlated. Our model incorporates the power delay profile of the channel, but neglects shadowing. These assumptions on the propagation scenario are typical for cellular suburban deployments. In the following M_B, M_S, M_R and M_T denote the number of antennas at the BTS, SU, receiver, and transmitter, respectively. Clearly, in the uplink $M_R = M_B, M_T = M_S$ and in the downlink $M_R = M_S$ and $M_T = M_B$.

Channel. Following [9, 10] the delay spread can be modeled by assuming that there are L significant scatterer clusters, and that each of the paths emanating from within the same scatterer cluster experiences the same delay, i.e., the delay equals τ_l for all the paths originating from the l-th cluster ($l = 0, 1, ..., L-1$). With $\mathbf{x}(t)$ denoting the $M_T \times 1$ transmitted signal vector and $\mathbf{y}(t)$ the $M_R \times 1$ received signal vector, respectively, we can therefore write $\mathbf{y}(t) = \sum_{l=0}^{L-1} \mathbf{H}_l \, \mathbf{x}(t-\tau_l)$ with the $M_R \times M_T$ complex-valued random matrices $\mathbf{H}_l$ denoting the l-th tap of the stochastic matrix-valued channel impulse response. Throughout this paper we assume that the elements of the $\mathbf{H}_l$ are (possibly correlated) circularly symmetric complex gaussian random variables[2]. Each scatterer cluster has a mean angle of arrival at the BTS $\bar{\theta}_l$, an angular spread δ_l, and a (complex) path gain β_l. We furthermore assume that the *individual scatterer clusters are uncorrelated.*

Array Geometry. We assume a uniform linear array (ULA) at both the BTS and the SU. The relative antenna spacing is denoted as $\Delta = \frac{d}{\lambda}$, where d is the absolute antenna spacing and $\lambda = c/f_c$ is the wavelength of a narrowband signal with center frequency f_c.

This work was supported in part by FWF grant J1629-TEC. H. Bölcskei is on leave from the Dept. of Communications, Vienna University of Technology, Vienna, Austria. A. Paulraj is on part-time leave at Gigabit Wireless Inc., 1916B Old Middlefield Way, Mountain View, CA.

[1] This statement will be made more clear in Sec. 2.

[2] A circularly symmetric complex gaussian random variable is a random variable $z = (x + jy) \sim \mathcal{CN}(0, \sigma^2)$, where x and y are i.i.d. $\mathcal{N}(0, \sigma^2/2)$.

Fading Statistics. In the following we assume that there is no line-of-sight connection between the BTS and the SU and that the angle of arrival for the l-th path cluster at the BTS is Gaussian distributed around the mean angle of arrival $\bar{\theta}_l$, i.e., the actual angle of arrival is given by $\theta_l = \bar{\theta}_l + \hat{\theta}_l$ with $\hat{\theta}_l \sim \mathcal{N}(0, \sigma_{\theta_l})$. The variance σ_{θ_l} is proportional to the angular spread δ_l and hence the scattering radius of the l-th path cluster. The correlation matrix of the k-th column of the zero mean matrix $\mathbf{H}_l$ given by $\mathbf{R}_l = \mathcal{E}\{\mathbf{h}_{l,k}\mathbf{h}_{l,k}^H\}$ is independent of k, or equivalently the fading statistics are the same for all transmit antennas. Defining $\rho_l(s\Delta, \bar{\theta}_l, \sigma_{\theta_l}) = \mathcal{E}\{h_{l,k}^{(r)} h_{l,k}^{(r+s)^*}\}$ for $l = 0, 1, ..., L-1$, $k = 0, 1, ..., M_T - 1$ to be the fading correlation between two BTS antenna elements spaced $s\Delta$ wavelengths apart, the correlation matrix $\mathbf{R}_l$ ($l = 0, 1, ..., L-1$) can be written as

$$[\mathbf{R}_l]_{m,n} = |\beta_l|^2 \rho_l((n-m)\Delta, \bar{\theta}_l, \sigma_{\theta_l}), \qquad (1)$$

where we have absorbed the power delay profile of the channel into the correlation matrices. Throughout this paper we will use $|\beta_0|^2 = 1$. For small angular spread the correlation function in (1) is given by [9]

$$\rho_l(s\Delta, \bar{\theta}_l, \sigma_{\theta_l}) \approx e^{-j2\pi s\Delta\cos(\bar{\theta}_l)} e^{-\frac{1}{2}(2\pi s\Delta sin(\bar{\theta}_l)\sigma_{\theta_l})^2}.$$

We note that although this approximation is accurate only for small angular spread, it does provide the correct trend for large angular spread, namely uncorrelated spatial fading. For $\sigma_{\theta_l} = 0$ the correlation matrix $\mathbf{R}_l$ collapses to a rank-1 matrix and can be written as $\mathbf{R}_l = |\beta_l|^2 \mathbf{a}(\bar{\theta}_l)\mathbf{a}^H(\bar{\theta}_l)$ with the array response vector of the ULA given by

$$\mathbf{a}(\theta) = [1 \;\; e^{j2\pi\Delta\cos(\theta)} \;\; ... \;\; e^{j2\pi(M_R-1)\Delta\cos(\theta)}]^T. \qquad (2)$$

Uplink Channel Model. Since fading is spatially uncorrelated at the SU, in the uplink different columns of $\mathbf{H}_l$ will be uncorrelated whereas different rows will be correlated. Factoring the $M_B \times M_B$ correlation matrix $\mathbf{R}_l$ according to $\mathbf{R}_l = \mathbf{R}_l^{1/2}\mathbf{R}_l^{H/2}$, where $\mathbf{R}_l^{1/2}$ is of size $M_B \times M_B$, the $M_B \times M_S$ matrices $\mathbf{H}_l$ can be written as

$$\mathbf{H}_l = \mathbf{R}_l^{1/2}\mathbf{H}_{w,l}, \quad l = 0, 1, ..., L-1 \qquad (3)$$

with the $\mathbf{H}_{w,l}$ being uncorrelated $M_B \times M_S$ matrices with i.i.d. $\mathcal{CN}(0, 1)$ entries.

Downlink Channel Model. In the downlink spatial fading is uncorrelated at the receive antennas. Consequently different rows of $\mathbf{H}_l$ will be uncorrelated and different columns will be correlated. Employing the same assumptions on the scatterer statistics as in the uplink, the $M_S \times M_B$ matrices $\mathbf{H}_l$ can be decomposed as

$$\mathbf{H}_l = \mathbf{H}_{w,l}\mathbf{R}_l^{T/2}, \quad l = 0, 1, ..., L-1, \qquad (4)$$

where the $\mathbf{H}_{w,l}$ are $M_S \times M_B$ matrices of i.i.d. $\mathcal{CN}(0, 1)$ random variables.

Differences to the Parametric Channel Model. In the parametric channel model proposed in [4, 8] each tap $\mathbf{H}_l$ can be written as

$$\mathbf{H}_l = \beta_l \, \mathbf{a}_R(\bar{\theta}_{R,l})\mathbf{a}_D^T(\bar{\theta}_{D,l}), \qquad l = 0, 1, ..., L-1,$$

where β_l denotes the path gain, $\bar{\theta}_{R,l}$ and $\bar{\theta}_{D,l}$ are the angle-of-arrival and angle-of-departure, respectively, of the l-th path, and $\mathbf{a}_R(\theta)$ and $\mathbf{a}_D(\theta)$ are the $M_R \times 1$ and $M_T \times 1$ receive and transmit array response vectors (cf. (2)), respectively. Note that here $\mathbf{H}_l$ will always have rank 1 irrespectively of the angular spread. From (3) and (4) it follows that in our space-time channel model the rank of the matrices $\mathbf{H}_l$ is controled by the fading correlation at the BTS. For large angular spread $\mathbf{H}_l$ will have full rank, whereas for small angular spread the rank of $\mathbf{H}_l$ will decrease. The space-time channel model proposed in this paper is therefore more flexible than the parametric channel model [4, 8] and seems to be a more adequate description of a real-world scattering environment. The capacity obtained using our channel model can be as low as the capacity predicted by the parametric channel model, but will in the presence of angle spread in general be significantly higher (see Simulation Example 2).

3. OFDM-BASED SPATIAL MULTIPLEXING

Spatial multiplexing [1], also referred to as BLAST technology [2, 5] has the potential to dramatically increase the capacity of wireless radio links with no additional power or bandwidth consumption.

Let us assume that the delay spread of the matrix channel is L taps, i.e., the channel transfer matrix can be written as $\mathbf{H}(e^{j2\pi\theta}) = \sum_{l=0}^{L-1} \mathbf{H}_l \, e^{-j2\pi l\theta}$, where now $\mathbf{H}_l$ denotes the discrete-time channel impulse response obtained by sampling the continuous-time impulse response at a rate of $\frac{1}{W}$, where W is the bandwidth of the analog OFDM-signal. In an OFDM-based spatial multiplexing system the (possibly coded) data stream corresponding to the i-th transmit antenna is first passed through an OFDM modulator and then transmitted from that antenna. The OFDM modulator applies an N-point IFFT to N data symbols and then prepends the CP (which is a copy of the last L samples of the symbol) to the symbol, so that the overall OFDM symbol length is $M = N + L$. Note that this transmission takes place simultaneously from all M_T transmit antennas. In the receiver, the individual signals are passed through an OFDM demodulator, separated, and then decoded. The OFDM demodulator first discards the CP and then applies an FFT. Organizing the transmitted data symbols into frequency vectors $\mathbf{c}_k = [c_k^{(0)} \; c_k^{(1)} \; ... \; c_k^{(M_T-1)}]^T$ with $c_k^{(i)}$ denoting the data symbol transmitted from the i-th antenna on the k-th tone, it can be shown that

$$\hat{\mathbf{c}}_k = \mathbf{H}(e^{j2\pi\frac{k}{N}})\mathbf{c}_k + \mathbf{n}_k, \quad k = 0, 1, ..., N-1, \qquad (5)$$

where $\hat{\mathbf{c}}_k$ denotes the reconstructed data vector for the k-th tone, and $\mathbf{n}_k$ is additive white gaussian noise satisfying

$$\mathcal{E}\{\mathbf{n}_k\mathbf{n}_l^H\} = \sigma_n^2 \mathbf{I}_{M_R}\delta[k-l], \qquad (6)$$

where $\mathbf{I}_{M_R}$ is the identity matrix of size M_R.

4. CAPACITY

In this section, we shall compute the capacity of an OFDM-based spatial multiplexing system using the space-time channel model introduced in Sec. 2. We note that since the channel is random its capacity will be a random variable. Furthermore, we emphasize that only in the limiting case where the number of tones in the OFDM system goes to infinity the capacity of the OFDM-based spatial multiplexing system approaches the exact capacity of the underlying space-time channel.

We start by stacking the vectors $\hat{\mathbf{c}}_k, \mathbf{c}_k$, and $\mathbf{n}_k$ according to $\hat{\mathbf{c}} = [\hat{\mathbf{c}}_0^T \; \hat{\mathbf{c}}_1^T \; ... \; \hat{\mathbf{c}}_{N-1}^T]^T$, $\mathbf{c} = [\mathbf{c}_0^T \; \mathbf{c}_1^T \; ... \; \mathbf{c}_{N-1}^T]^T$, and $\mathbf{n} = [\mathbf{n}_0^T \; \mathbf{n}_1^T \; ... \; \mathbf{n}_{N-1}^T]^T$, where $\hat{\mathbf{c}}$ and $\mathbf{n}$ are $M_R N \times 1$ vectors and $\mathbf{c}$ is an $M_T N \times 1$ vector. Note that (6) implies that the noise vector $\mathbf{n}$ is white, i.e., $\mathcal{E}\{\mathbf{n}\mathbf{n}^H\} = \sigma_n^2 \mathbf{I}_{M_R N}$. We furthermore define the $NM_R \times NM_T$ block-diagonal matrix

$$\mathbf{H} = \text{diag}\{\mathbf{H}(e^{j2\pi\frac{k}{N}})\}_{k=0}^{N-1}.$$

With these definitions the input-output relation (5) can be rewritten as

$$\hat{\mathbf{c}} = \mathbf{H}\mathbf{c} + \mathbf{n}. \qquad (7)$$

In the following we assume that for each channel use an independent realization of the random channel impulse response matrices $\mathbf{H}_l$ is drawn and that the channel remains constant within one channel use. Using (7) the capacity (in bps/Hz) of the OFDM-based spatial multiplexing system (assuming that the channel is unknown at the transmitter and perfectly known at the receiver) under an average transmitter power constraint is given by[3] [11]

$$C = \frac{1}{N}\sum_{k=0}^{N-1} \log\left[\det\left(\mathbf{I}_{M_R} + \rho\mathbf{H}(e^{j2\pi\frac{k}{N}})\mathbf{H}^H(e^{j2\pi\frac{k}{N}})\right)\right],$$

where $\rho = \frac{P}{M_T N \sigma_n^2}$ with P denoting the maximum overall transmit power. In [11] it was shown that the uplink capacity distribution is equal to the downlink capacity distribution. In the following we shall therefore not distinguish between the two cases and employ the notation for the uplink case. The capacity distribution was derived in [11] as[4]

$$C \sim \frac{1}{N}\sum_{k=0}^{N-1} \log\left[\det\left(\mathbf{I}_{M_B} + \rho\mathbf{D}_k\mathbf{V}_k^H\mathbf{H}\mathbf{H}^H\mathbf{V}_k\mathbf{D}_k^H\right)\right],$$

where the following definitions have been used

$$\mathbf{R}^{1/2}(\mathbf{W}_k \otimes \mathbf{I}_{M_B}) = \mathbf{U}_k\mathbf{D}_k\mathbf{V}_k^H \tag{8}$$

with $\otimes$ denoting the Kronecker product, $\mathbf{R}^{1/2} = [\mathbf{R}_0^{1/2}\ \mathbf{R}_1^{1/2}\ \ldots\ \mathbf{R}_{L-1}^{1/2}]$, $\mathbf{W}_k = \mathrm{diag}\{e^{-j2\pi\frac{k}{N}l}\}_{l=0}^{L-1}$, and $\mathbf{H} = [\mathbf{H}_{w,0}^T\ \mathbf{H}_{w,1}^T\ \ldots\ \mathbf{H}_{w,L-1}^T]^T$. Next, noting that the unitarity of the matrices $\mathbf{V}_k$ implies that [12] $\mathbf{V}_k^H\mathbf{H}\mathbf{H}^H\mathbf{V}_k \sim \mathbf{H}\mathbf{H}^H$, we get

$$C \sim \frac{1}{N}\sum_{k=0}^{N-1} \log\left[\det\left(\mathbf{I}_{M_B} + \rho\mathbf{D}_k\mathbf{H}\mathbf{H}^H\mathbf{D}_k^H\right)\right], \tag{9}$$

which using

$$\mathbf{D}_k = [\mathbf{\Lambda}_k\ \underbrace{\mathbf{0}_{M_B}\ \ldots\ \mathbf{0}_{M_B}}_{(L-1)\text{ times}}] \quad \text{with} \quad \mathbf{\Lambda}_k = \mathrm{diag}\{\lambda_{k,l}\}_{l=0}^{M_B-1} \tag{10}$$

finally results in

$$C \sim \frac{1}{N}\sum_{k=0}^{N-1} \log\left[\det\left(\mathbf{I}_{M_B} + \rho\mathbf{\Lambda}_k\mathbf{H}_w\mathbf{H}_w^H\mathbf{\Lambda}_k^H\right)\right]. \tag{11}$$

Here, for the sake of simplicity, we have set $\mathbf{H}_{w,0} = \mathbf{H}_w$. From (11) it follows that the capacity of the delay spread matrix channel is given by the sum of the capacities of N i.i.d. gaussian $M_B \times M_S$ channels followed by a frequency-dependent attenuation at each receive antenna.

Bounds on capacity. We shall next derive bounds on expected capacity and the capacity distribution, which can be used to conveniently check the influence of physical parameters and system parameters on capacity without performing Monte-Carlo simulations. An upper bound on expected capacity is given by [11]

$$\mathcal{E}\{C\} \leq \frac{1}{N}\sum_{k=0}^{N-1}\sum_{l=0}^{r_k-1} \log\left(1 + \rho M_S\,|\lambda_{k,l}|^2\right), \tag{12}$$

where r_k denotes the rank of $\mathbf{\Lambda}_k$ (or equivalently the number of nonzero entries in $\mathbf{\Lambda}_k$). Eq. (12) shows that the expected capacity is upper-bounded by the (normalized) sum of the capacities of N spatial subchannels $k = 0, 1, \ldots, N-1$, which themselves consist of r_k parallel scalar subchannels with power gain $M_S|\lambda_{k,i}|^2$.

We shall next derive the distribution of lower and upper bounds on (11). The techniques used below have mostly been borrowed from [7], especially the idea of using the QR-decomposition of the white channel transfer matrix $\mathbf{H}_w$ in this context is taken from [7]. In the following we assume that $M_S \geq M_B$. With the QR-decomposition of the $M_S \times M_B$ matrix $\mathbf{H}_w^H$ given by $\mathbf{H}_w^H = \mathbf{Q}\mathbf{R}_w$, we obtain the distribution of a capacity lower bound C_l as [11]

$$C_l \sim \frac{1}{N}\sum_{k=0}^{N-1}\sum_{l=0}^{r_k-1} \log\left(1 + \rho\,|\lambda_{k,l}|^2|r_{l,l}|^2\right), \tag{13}$$

where $r_{l,l}$ denotes the entries on the main diagonal of $\mathbf{R}_w$. The distribution of a capacity upper bound C_u follows as [11]

$$\begin{aligned} C_u \quad &\sim \quad \frac{1}{N}\sum_{k=0}^{N-1}\sum_{l=0}^{r_k-1} \log[1 + \rho\,(|\lambda_{k,l}|^2|r_{l,l}|^2 \\ &+ \sum_{m=l+1}^{r_k-1} |\lambda_{k,m}|^2|r_{l,m}|^2)]. \end{aligned}$$

Now, since the $|r_{l,l}|^2$ are independent and chi-squared distributed with $M_S - l$ degrees of freedom [12] it follows that the capacity of the delay-spread channel is lower bounded by the sum of the capacities of $\sum_{k=0}^{N-1} r_k$ subchannels, whose power gains consist of a deterministic factor $|\lambda_{k,l}|^2$ and a stochastic factor given by independent chi-squared random variables with degrees of freedom $M_S, M_S-1, \ldots, M_S-r_k+1$ for $k = 0, 1, \ldots, N-1$. A similar interpretation can be given for the upper bound.

5. SIMULATION RESULTS

Based on (11) we can estimate the capacity distribution (and hence expected capacity and outage capacity) using a Monte Carlo method. In each Monte Carlo run an $M_B \times M_S$ i.i.d. gaussian matrix $\mathbf{H}_w$ is generated and the corresponding capacity C is computed according to (11). Outage capacity is an important measure for channel capacity in quasi-static fading environments. Specifically, an outage capacity of C_q states that the channel capacity is less than C_q with probability q, i.e., $\mathrm{Prob}[C > C_q] = 1 - q$. In our simulations we consider the case $q = 0.1$. In every simulation example 1,000 realizations of the matrix $\mathbf{H}_w$ were used. Unless specified otherwise, the power delay profile was taken to be exponential, the OFDM-system parameters were chosen to be $N = 512, M = 576$, the relative antenna spacing was $\Delta = 0.5$, and $\mathrm{SNR} = M_T\rho = \frac{P}{N\sigma_n^2}$.

Simulation Example 1. In the first simulation example, we study the impact of delay spread on channel capacity. The number of antennas was $M_B = M_S = 4$. The mean angles of arrival satisfied $\bar{\theta}_l \in [\frac{\pi}{3}, \frac{2\pi}{3}]$ and the angular spread of the individual scatterer clusters was chosen such that $\sigma_{\theta,l} \in [0, \frac{\pi}{4}]$. Fig. 1 shows the expected capacity and outage capacity as a function of SNR for different amounts of delay spread assuming that each channel tap corresponds to an independent scatterer. It is clearly seen that both the expected capacity and outage capacity increase for increasing channel delay spread, which corroborates the intuition that delay spread is a contributor to capacity.

Simulation Example 2. In the second simulation example, we compare the capacity obtained using the stochastic parametric channel model proposed in [4, 8] with the capacity predicted by the space-time channel model proposed in this paper. In both cases we assumed that the delay spread is $L = 10$ and that each channel impulse response sample corresponds to an independent scatterer cluster. The parameters for our space-time channel model were generated as in Simulation Example 1. In the case of the parametric channel model in each Monte Carlo run the angles of departure and the angles of arrival were drawn from two independent gaussian distributions such that the total angle spread was the same as in the case of the space-time

[3]Throughout the paper all logarithms are to the base 2.

[4]The notation $x \sim y$ means that the distribution of the random variable x is equal to the distribution of the random variable y.

channel model. For SNR = 20dB, Fig. 2 shows the expected capacity obtained from the two different channel models as a function of the number of antennas $M_B = M_S$. It is clearly seen that our space-time channel model predicts much higher capacities than the parametric channel model (see the comments at the end of Sec. 2).

Simulation Example 3. In the last simulation example, we compute the capacity complementary cdf (ccdf) corresponding to the *typical urban* channel taken from the GSM recommendations. The spatial fading statistics were chosen as in Simulation Example 1. For a bandwidth of 5MHz, the delay spread is 25 samples in accordance with the GSM recommendations. Furthermore, the number of independent scatterer clusters is 12. Fig. 3 shows the capacity ccdf at an SNR of 20dB for different numbers of antennas. The results for the hilly terrain channel are very similar. We found that an OFDM-based spatial multiplexing system employing $M_B = M_S = 4$ antennas has an expected capacity of roughly 19bps/Hz at an SNR of 20dB in a typical urban environment. Taking into account the loss in spectral efficiency due to the CP this capacity corresponds to an (expected) data rate of approximately 80Mbps.

6. CONCLUSION

Based on an abstract model for stochastic spatial delay spread channels, we derived an expression for the capacity of OFDM-based spatial multiplexing systems. We provided a Monte-Carlo method for estimating the capacity cdf, expected capacity, and outage capacity, and we established bounds on capacity. We furthermore showed that the capacity of an OFDM-based spatial multiplexing system is equal to the sum of the capacities of N spatial channels which consist of the same white random channel followed by a frequency-dependent attenuation at each receive antenna. Our simulation results show that delay spread and angle spread significantly boost the capacity of multi-antenna systems.

7. REFERENCES

[1] A. J. Paulraj and T. Kailath, "Increasing capacity in wireless broadcast systems using distributed transmission/directional reception," *U. S. Patent*, no. 5,345,599, 1994.

[2] G. J. Foschini, "Layered space-time architecture for wireless communication in a fading environment when using multi-element antennas," *Bell Labs Tech. J.*, pp. 41–59, Autumn 1996.

[3] I. E. Telatar, "Capacity of multi-antenna gaussian channels," Tech. Rep. #BL0112170-950615-07TM, AT & T Bell Laboratories, 1995.

[4] G. G. Raleigh and J. M. Cioffi, "Spatio-temporal coding for wireless communication," *IEEE Trans. Comm.*, vol. 46, no. 3, pp. 357–366, 1998.

[5] G. J. Foschini and M. J. Gans, "On limits of wireless communications in a fading environment when using multiple antennas," *Wireless Personal Communications*, vol. 6, pp. 311–335, 1998.

[6] T. L. Marzetta and B. M. Hochwald, "Capacity of a mobile multiple-antenna communication link in Rayleigh flat fading," *IEEE Trans. Inf. Theory*, vol. 45, pp. 139–157, Jan. 1999.

[7] D. Shiu, G. J. Foschini, M. J. Gans, and J. M. Kahn, "Fading correlation and its effect on the capacity of multi-element antenna systems," *IEEE Trans. Comm.*, 1999. to appear.

[8] G. G. Raleigh and V. K. Jones, "Multivariate modulation and coding for wireless communication," *IEEE J. Sel. Areas Comm.*, vol. 17, no. 5, pp. 851–866, 1999.

[9] D. Asztély, "On antenna arrays in mobile communication systems: Fast fading and GSM base station receiver algorithms," Tech. Rep. IR-S3-SB-9611, Royal Institute of Technology, Stockholm, Sweden, March 1996.

[10] J. Fuhl, A. F. Molisch, and E. Bonek, "Unified channel model for mobile radio systems with smart antennas," *IEE Proc.-Radar, Sonar Navig.*, vol. 145, pp. 32–41, Feb. 1998.

[11] H. Bölcskei, D. Gesbert, and A. J. Paulraj, "On the capacity of wireless systems employing OFDM-based spatial multiplexing," *IEEE Trans. Comm.*, Oct. 1999. submitted.

[12] R. J. Muirhead, *Aspects of Multivariate Statistical Theory*. Wiley, 1982.

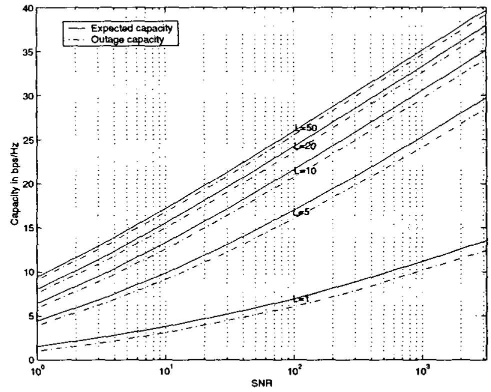

Fig. 1. Expected capacity and outage capacity in bps/Hz as a function of SNR for $L = 1, 5, 10, 20$ and 50.

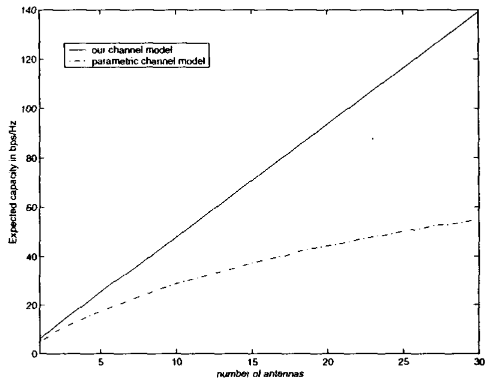

Fig. 2. Comparison of the expected capacity obtained using the parametric channel model from [4, 8] and the space-time channel model proposed in this paper.

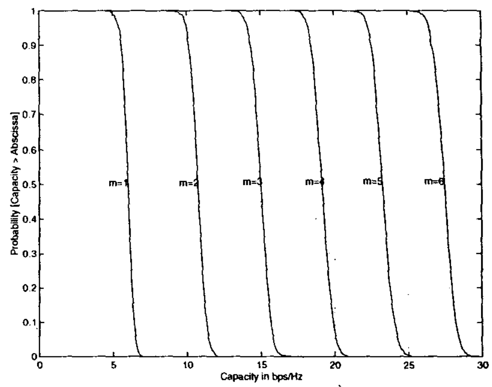

Fig. 3. Capacity ccdfs for the GSM typical urban channel at an SNR of 20dB for different numbers of antennas $m = M_B = M_S$.